



The oxygen sensing mechanism of a trifluoromethyl-substituted cyclometalated platinum(II) complex

Yu Ning^a, Xuedan Song^{b,*}, Heming Zhang^b, Tianqing Liu^a, Ce Hao^b

^a School of Chemical Engineering, Dalian University of Technology, Dalian, Liaoning Province 116024, China

^b State Key Laboratory of Fine Chemicals, Dalian University of Technology, Dalian, Liaoning Province 116024, China

ARTICLE INFO

Keywords:

Oxygen sensing
Luminescence mechanism
Quenching

ABSTRACT

Trifluoromethyl-substituted cyclometalated platinum(II) (TSCP) is a useful material for oxygen molecule detection and determination. Through quantum chemical computation, we propose a quenching mechanism to explain the nature of oxygen sensing. The luminescence mechanism of TSCP involves phosphorescent emission and the TSCP-O₂ complex internal conversion. By applying the density functional theory (DFT) method, we computed the frontier molecular orbitals and electron configurations of TSCP and the TSCP-O₂ complex. In addition, using the time-dependent density functional theory (TDDFT) method, we computed the excited energies and geometric optimization of the excited state of TSCP and the TSCP-O₂ complex. According to the computation results, the luminescence of TSCP is due to localized excitation, while that of the TSCP-O₂ complex is due to delocalized excitation. We computed the radiative and non-radiative rate constants of TSCP and the TSCP-O₂ complex and elucidated their photophysical processes. For TSCP, after excitation, first the electron jumped from the S₁ to T₁ state by intersystem crossing, and eventually back to the S₀ state by phosphorescence emission. Instead, for the TSCP-O₂ complex without spin flip, the electron jumped directly from the T₁ to T₀ state by internal conversion.

1. Introduction

Oxygen is a vital element for life on earth and plays an essential role in life activities. The detection and determination of oxygen is widely used in numerous fields, such as industry, biology, environment, medical care, food processing, etc. [1–5] Traditional measurement methods consist mainly of standard iodometry and Clark electrode [6,7]. However, the operation of the former is complicated and time-consuming [8], while the latter is likely to be affected by electromagnetic signals during operation [9]. Accordingly, these two traditional methods are limited in application. Recently, a photochemical oxygen sensing method has attracted increasing attention due to its advantages of high sensitivity, good selectivity, and non-consumption of analyte [10,11]. Additionally, it is resistant to electromagnetic interference, so the signals can be transmitted over a long distance, which makes it a good candidate for remote control and on-line monitoring [12,13].

Among a variety of oxygen sensing materials, the platinum complex stands out with its characteristics of long luminescence lifetime and high luminescent quantum yield [14–16]. Liu et al. synthesized a series of cyclometalated platinum complexes with intensive phosphorescent

emission at room temperature [17–19]. To explain the mechanism of oxygen sensing of cyclometalated platinum complexes, the dynamic collision method is usually adopted in experimental research [10,20]. Specifically, when the excited state of the luminescent material (LM) collides with the triplet state of an oxygen molecule, the former changes into the ground state and the latter into a singlet. However, the oxygen molecule is not luminescent, and its stable existence state is not in a singlet state either, which obviously conflicts with reality. Thus, in this paper, we propose a novel quenching procedure to elucidate the oxygen sensing mechanism.

From the various complexes synthesized by Liu and coworkers, we chose a trifluoromethyl-substituted cyclometalated platinum(II) (TSCP) as the study target [18]. Using the method of quantum chemistry computation, we adopted the density functional theory (DFT) method and time-dependent density functional theory (TDDFT) method to investigate the configuration and characteristics of the TSCP-O₂ complex with the appropriate functional and basis set. Based on the frontier molecular orbitals and electronic configuration, we explored the change of the luminescence mechanism before and after the combination of TSCP and O₂, examined the relationship between the hydrogen bonding in excited states and the luminescence property of TSCP, and elucidated

* Corresponding author.

E-mail address: song@dlut.edu.cn (X. Song).

<https://doi.org/10.1016/j.comptc.2018.10.008>

Received 23 July 2018; Received in revised form 17 October 2018; Accepted 23 October 2018

Available online 25 October 2018

2210-271X/ © 2018 Elsevier B.V. All rights reserved.

the mechanism of oxygen molecular recognition and chemical sensing of TSCP. Finally, each transition of the photophysical process of TSCP and the TSCP-O₂ complex was elucidated based on the time-dependent perturbation theory and Fermi's golden rule.

2. Computational details

2.1. Computation methodology

The Gaussian 09 software program was used to perform the computations [21]. For the ground states of TSCP and the two TSCP-O₂ complexes, the optimization of their geometric structures was performed by the DFT method, and their excited states by the TDDFT method. The functional theory was the B3LYP [22] and the basis sets were hybrid, where the 6-311(d) basis set was used for C, H, O, N and F atoms and LANL2DZ for Pt atom [23]. Moreover, the van der Waals-density functional theory (vdW-DFT) method was used to calculate the geometry optimizations of TSCP-O₂ complexes. The scaling factor was set at 0.961 for the computation of the infrared (IR) spectra [24]. The computation of electronic configuration was performed using the ADF 2012 software program [25,26].

The Molecular Materials Property Prediction Package (MOMAP) is a software toolkit for the prediction of the properties of molecular materials. It focuses on luminescent properties and charge mobility properties [27]. In this paper, we used it to compute the radiative and non-radiative rate constants. For the TSCP, the phosphorescent radiative rate (k_p) and the intersystem crossing rate (k_{isc}) were computed, and then the photophysical processes were proposed based on the results. For TSCP-O₂ complex, the fluorescent radiative rate (k_f) and internal conversion rate (k_{ic}) were computed to elucidate the mechanism of oxygen sensing.

2.2. Computational model

The optimized and corresponding experimental values of the geometry parameters of TSCP are listed in Table 1, including bond length and bond angles. Additionally, the computed ultraviolet-visible (UV-vis) maximum absorption band was at 310 nm, which approximately corresponded to the experimental band was at 302 nm. The computed phosphorescent emission bands were at 428 nm and 588 nm (sh), while the experimental bands were at 510 nm and 538 nm (sh). Except for the phosphorescent emission bands, all the deviations were small, indicating that the functional theory and basis sets were reliable.

Generally, the ground state of molecular oxygen is a spin triplet. But the singlet molecular oxygen usually refers to the lowest excited electronic state [28,29]. Using the B3LYP functional and 6-311(d)/LANL2DZ hybrid basis sets, the relative energy of the singlet and triplet states of O₂, TSCP and TSCP-O₂ complex are listed in Table 2. The results revealed that the relative energy of the triplet and singlet

Table 1

The geometry parameters, UV-vis absorption spectrum and phosphorescence emission spectrum of TSCP and its corresponding experimental values.

	Exp. values [18]	Cal. values
<i>Bond length (Å)</i>		
Pt13-N4	2.003	2.02365
Pt13-C12	1.968	1.98567
Pt13-O18	2.081	2.14879
Pt13-O14	2.000	2.04942
<i>Bond angles (°)</i>		
C12-Pt13-N4	81.621	81.01978
O18-Pt13-O14	92.478	90.05245
UV-vis maximum absorption (nm)	302	310
Phosphorescent emission ^a spectrum (nm)	510, 538 (sh)	428, 588 (sh)

^a sh = shoulder.

Table 2

The relative energy of singlet and triplet states of O₂, TSCP and the TSCP-O₂ complex.

Relative energy (kcal/mol)	O ₂	TSCP	The TSCP-O ₂ complex
Singlet	39.3	0	38.4
Triplet	0	56.2	0

molecular oxygen is 39.3 kcal/mol. And the energy of the triplet is lower than that of the singlet state, which means that the ground state of molecular oxygen is a triplet (T₀). Similarly, the ground state of TSCP is a singlet (S₀). After the combination of O₂ and TSCP, the ground state of the TSCP-O₂ complex also has two states, namely a singlet and a triplet. From the data presented in Table 2, we can figure out that the ground state of the TSCP-O₂ complex is a triplet (T₀).

The geometric structures of TSCP and the TSCP-O₂ complex are shown in Fig. 1. The combination between TSCP and O₂ produces two complexes, namely Complex 1 and Complex 2, and the geometric structures are shown in Fig. 1(b) and Fig. 1(c), respectively. As the energy difference between them is 0.14 kcal/mol, which is less than 2 kcal/mol, either of them can be used for subsequent computation. Considering the bifurcated hydrogen bond in the structure, Complex 1 was chosen as the computational target in this paper and is denoted as the TSCP-O₂ complex. According to the data shown in Table 2, the triplet state of the TSCP-O₂ complex is more stable.

3. Results and discussion

3.1. Variation of the luminescence mechanism

The luminescence mechanism of the LMs is closely related to the frontier molecular orbitals and electronic configuration, especially the highest occupied molecular orbital (HOMO) and the lowest unoccupied molecular orbital (LUMO). For this reason, the DFT method is employed to calculate the HOMO/LUMO of TSCP and the TSCP-O₂ complex in this paper.

3.1.1. The luminescence mechanism of TSCP

In this study, the TSCP emitted phosphorescence at room temperature. The frontier molecular orbitals and electronic configuration of TSCP are shown in Fig. 2. There was no single electron in the frontier molecular orbital of TSCP, which implied that its ground state was certainly a singlet state. The LUMO of TSCP consisted of C (1p), O (1p), N (1p) and Pt (3d) atoms and the contribution of each atom orbital was 78.08, 2.09, 17.18 and 5.47%, respectively. While the HOMO of TSCP consisted of C (1p), O (1p), N (1p) and Pt (3d) with a contribution of 51.29, 5.87, 2.96 and 33.20%, respectively. Thus, during the excitation process, the charge transition of TSCP could be depicted as intramolecular $\pi(\text{TSCP}) \rightarrow \pi^*(\text{TSCP})$. As a result, the luminescence mechanism of TSCP was due to localized excitation.

3.1.2. The luminescence mechanism of the TSCP-O₂ complex

The frontier molecular orbitals and electronic configuration of the TSCP-O₂ complex are shown in Fig. 3 and the contribution of each atom orbital is listed in Table 3. The ground state of the TSCP-O₂ complex was a triplet, thereby implying that there were two single-electrons, and thus two pairs of LUMO and HOMO. The LUMO-A of the TSCP-O₂ complex was composed of C (1p), O (1p), N (1p) and Pt (3d) with a contribution from each atom orbital of 78.11, 2.09, 17.18 and 4.98%, respectively. The HOMO-A was composed of C (1p), O (1p), N (1p) and Pt (3d) with a contribution from each orbital of 51.28, 5.86, 2.95 and 33.19%, respectively. The LUMO-B consisted entirely of O (1p), and HOMO-B consisted of C (1p), O (1p), N (1p) and Pt (3d) with a contribution from the orbitals of 51.21, 5.85, 2.94 and 33.17%, respectively. Thus, during the excitation process, the charge transition of the

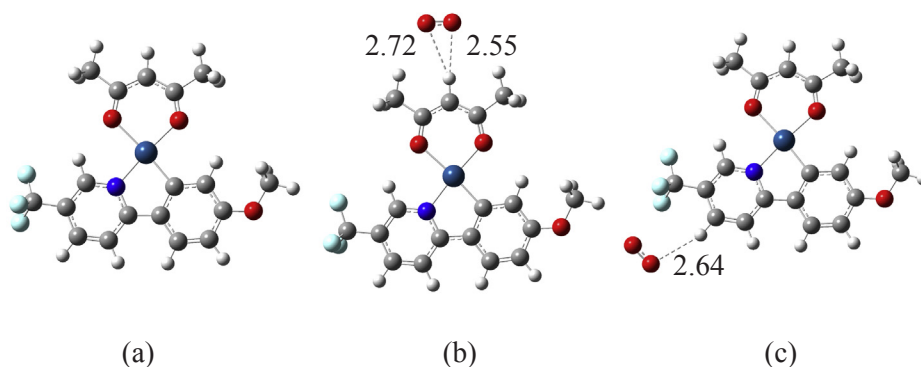


Fig. 1. The geometric structures of (a) TSCP, (b) TSCP-O₂ complex 1 and (c) the TSCP-O₂ complex 2. (C: grey, H: white, N: blue, O: red, F: light blue, Pt: dark blue.)

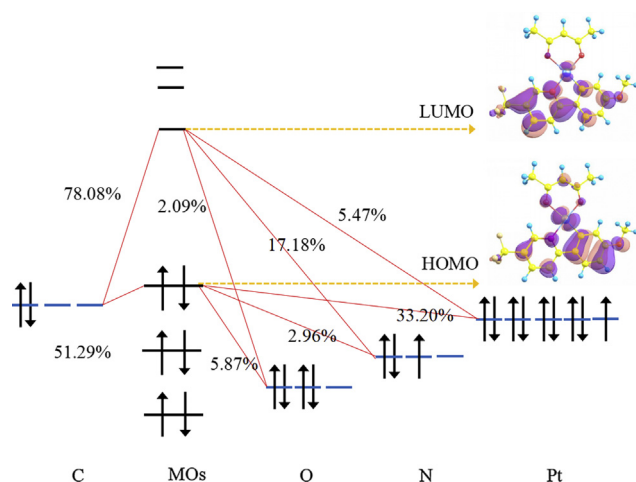


Fig. 2. The frontier molecular orbitals and electron configuration of TSCP.

TSCP-O₂ complex could be depicted as $\pi(\text{TSCP}) \rightarrow \pi^*(\text{TSCP})$ of group A and $\pi(\text{TSCP}) \rightarrow \pi^*(\text{O}_2)$ of group B.

As shown in Fig. 3, the electron density of the LUMO-B was totally distributed on the oxygen molecule, while the HOMO-B was totally distributed on the TSCP. This indicated that the luminescence mechanism of the TSCP-O₂ complex involved delocalized excitation, namely the electron transfer from the guest molecule to the ligand.

Comparing the frontier molecular orbitals and corresponding contributions before and after the combination of TSCP with an oxygen molecule, it is obvious that the oxygen molecule dramatically changed the composition of the frontier molecular orbitals of TSCP. Accordingly, the luminescence mechanism was altered from localized excitation to delocalized excitation.

3.2. Qualitative and quantitative analysis of the hydrogen bond

3.2.1. Qualitative analysis of the hydrogen bond

The behavior of the hydrogen bond in the excited state can dramatically affect the system and produce different electronic distribution in different excited states. Zhao et al. proposed that the strengthening of hydrogen bonds in the excited state would decrease the energy gap between the ground state and the first excited state, which could lead to a red shift in the spectrum. Specifically, a red shift in the spectrum indicates an strengthening of hydrogen bonds in the excited state. On the other hand, a blue shift indicates a weakening of hydrogen bonds in the excited state [30].

The electronic excitation energies and corresponding oscillation strengths of TSCP and the TSCP-O₂ complex are listed in Table 4. In each excited state, the electronic excitation energy of the TSCP-O₂ complex was lower than that of TSCP, which means a red shift in the

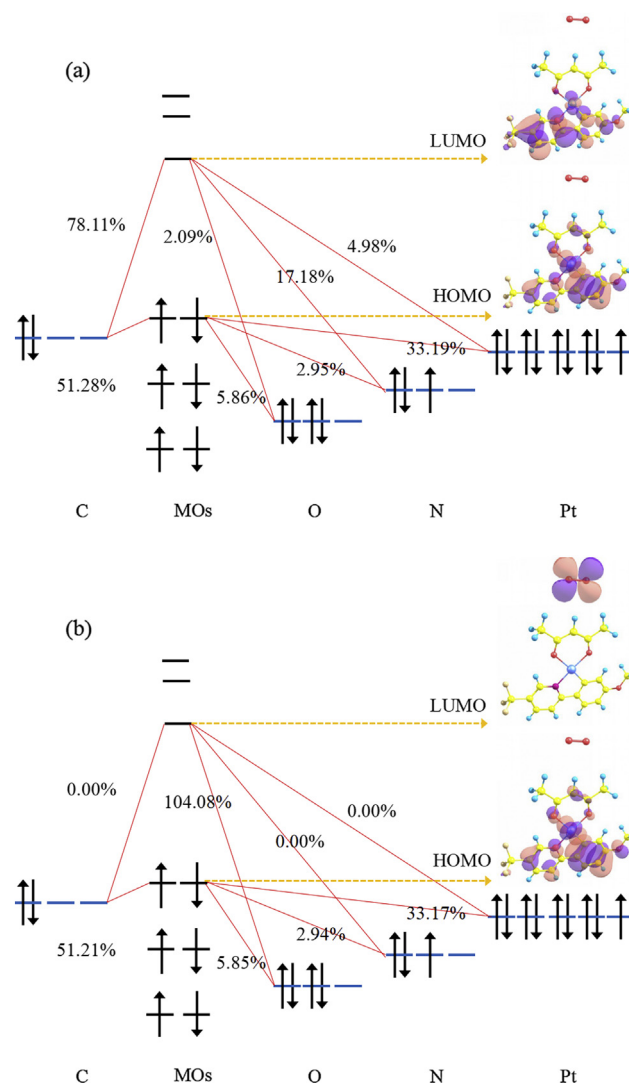


Fig. 3. The frontier molecular orbitals and electron configuration of the TSCP-O₂ complex (a) LUMO/HOMO-A, (b) LUMO/HOMO-B.

spectrum, or, in other words, the formation of hydrogen bonds was strengthened in the excited state.

3.2.2. Quantitative analysis of the hydrogen bond

The results of the computation of the hydrogen bond length, proton nuclear magnetic resonance (¹H NMR) spectroscopy and IR spectroscopy analysis are listed in Table 5. When TSCP combined with an oxygen molecule, a bifurcated hydrogen bond formed, as shown in

Table 3

The contribution of each atom orbital to LUMO/HOMO of the TSCP-O₂ complex.

	C (1p)	O (1p)	N (1p)	Pt (3d)
LUMO-A	78.11%	2.09%	17.18%	4.98%
HOMO-A	51.28%	5.86%	2.95%	33.19%
LUMO-B	0.00%	100%	0.00%	0.00%
HOMO-B	51.21%	5.85%	2.94%	33.17%

Table 4

The computed results of the electronic excitation energies (eV) and the corresponding oscillation strengths of TSCP and the TSCP-O₂ complex.

State	TSCP	The TSCP-O ₂ complex
S ₁ /T ₁	3.0282 (0.0704)	1.7673 (0.0000)
S ₂ /T ₂	3.4205 (0.0802)	1.8239 (0.0000)
S ₃ /T ₃	3.4431 (0.0032)	1.9386 (0.0000)
S ₄ /T ₄	3.6006 (0.0172)	1.9964 (0.0000)
S ₅ /T ₅	3.8150 (0.0937)	2.3710 (0.0001)
S ₆ /T ₆	3.8817 (0.0295)	2.4267 (0.0000)
S ₇ /T ₇	4.0348 (0.1758)	2.4696 (0.0000)
S ₈ /T ₈	4.0586 (0.0005)	2.4708 (0.0000)
S ₉ /T ₉	4.1825 (0.0874)	2.5248 (0.0000)
S ₁₀ /T ₁₀	4.1968 (0.0001)	2.9366 (0.0000)

Table 5

The hydrogen bonding length, ¹H NMR chemical shift and IR of the TSCP-O₂ complex in T₀ and T₁ states.

		T ₀ state	T ₁ state
Hydrogen bonding length (Å)	HB 1	2.74	2.22
	HB 2	2.73	2.24
¹ H NMR (ppm)		27.01	26.10
IR (cm ⁻¹)	Stretching of O=O	1654.68	1259.27

Fig. 1(b). The hydrogen bond length varied from 2.72 and 2.55 Å in the ground state to 2.21 and 2.21 Å in the excited state. Clearly, the hydrogen bond length was shorter in the excited state, which means that the hydrogen bond formation was strengthened in the excited state.

The ¹H NMR chemical shifts for the hydrogen-bonded proton was 27.01 ppm in the ground state and 26.10 ppm in the excited state, this up-field shift implied that the hydrogen bond increased in the excited state.

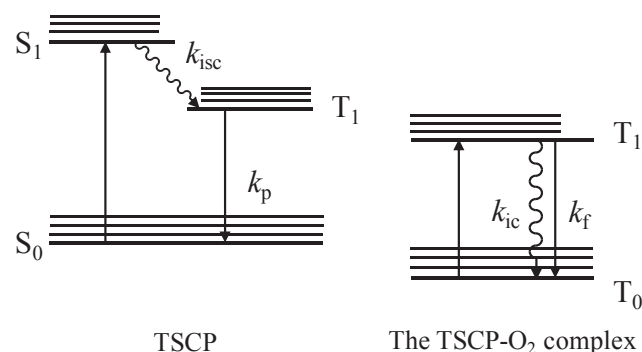
In addition, the results of the IR spectroscopy analysis of the TSCP-O₂ complex reveal that the stretching vibration of the hydrogen donor O=O molecule changed from 1654.68 cm⁻¹ in the ground state to 1259.27 cm⁻¹ in the excited state. Accordingly, the IR spectrum had a red shift in the excited state, which means that the hydrogen bond formation was strengthened in the excited state.

In short, the hydrogen bond formation was strengthened in the excited state, which had a great impact on the luminescence properties of TSCP. Thus, it was the hydrogen bond that led to the luminescence quenching in the experiment.

3.3. Analysis of the photophysical process

The luminescence mechanism of TSCP and the TSCP-O₂ complex can be explained using the Jablonski diagram [31] as shown in Fig. 4. The k_f , k_{ic} , k_p and k_{isc} were computed using the MOMAP software and the results are listed in Table 6.

For TSCP, according to the experimental phenomenon, the photophysical processes occurred through the following pathways. After S₀ → S₁ absorption, first, the electron arrived at the T₁ state via intersystem crossing (ISC). Then, it returned to the S₀ state with phosphorescent emission. According to the data in Table 6, the magnitude of k_p is 14 times larger than that of k_{isc} , which means that TSCP emits

**Fig. 4.** Jablonski diagram.**Table 6**

The radiative and nonradiative rate constants of TSCP and the TSCP-O₂ complex.

Rate constants (s ⁻¹)	TSCP	Rate constants (s ⁻¹)	The TSCP-O ₂ complex
k_p	2.0×10^5	k_f	6.1×10^2
k_{isc}	1.7×10^{-9}	k_{ic}	1.6×10^{10}

phosphorescence. The computed results are in good agreement with the experimental data.

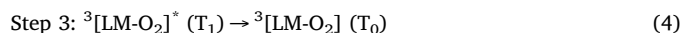
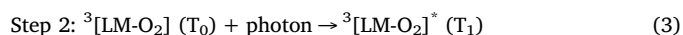
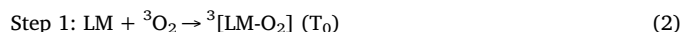
For the TSCP-O₂ complex, its ground state was a spin triplet (T₀) and the photophysical processes occurred via the following pathways. After T₀ → T₁ absorption, without spin flip, the electron directly returned to the T₀ state through internal conversion. According to the data in Table 6, the magnitude of k_{ic} is 8 times larger than that of k_f , thus we can conclude that the TSCP-O₂ complex undergoes internal conversion, and it is quite consistent with the quenching phenomenon observed experimentally.

3.4. The mechanism of oxygen sensing

To date, the dynamic collision method has always been adopted in reported studies in the literature to explain the mechanism of oxygen sensing. The dynamic mechanism considers that after the collision between the triplet excited state of the LM and the triplet oxygen molecule (³O₂), the former changes into the ground state and the latter into the singlet excited state. The mechanism can be briefly expressed as Eq. (1):



In this paper, according to the above computations, the luminescence mechanism process of oxygen sensing can be derived as Eq. (2)–(4):



This luminescence mechanism was proposed based on the above computations and the analysis of photophysical processes. After the combination with the oxygen molecule, TSCP first produced the triplet TSCP-O₂ complex, and then the TSCP-O₂ complex was excited to the triplet excitation state. Eventually, the TSCP-O₂ complex transitioned from the triplet excited state back to the ground state along with the internal conversion. The formation of hydrogen bonds promoted the combination between TSCP and O₂. As discussed above, the strengthening of the hydrogen bond formation in the excited state decreases the energy gap between the T₀ and T₁ state, thereby facilitating the internal conversion, which is why the luminescence quenching occurs in the experiment.

4. Conclusions

In this study, we computed the frontier molecular orbitals and the electronic configurations of TSCP and the TSCP-O₂ complex by applying the quantum chemistry computation method. Additionally, the luminescence mechanisms were elucidated. Specifically, for TSCP itself, the phosphorescence was caused by localized excitation and the charge transition was intramolecular $\pi(\text{TSCP}) \rightarrow \pi^*(\text{TSCP})$, while for the TSCP-O₂ complex, the luminescence mechanism was delocalized excitation and the charge transition were $\pi(\text{TSCP}) \rightarrow \pi^*(\text{TSCP})$ of group A and $\pi(\text{TSCP}) \rightarrow \pi^*(\text{O}_2)$ of group B, respectively. In addition, the strengthening of hydrogen bonds formation in the excited state led to the decrease of the energy gap between the ground and excited states, which favored internal conversion rather than luminescence. This is the reason why the phosphorescence was quenched by the molecular oxygen in the experiment.

In order to elucidate the photophysical processes before and after the combination of TSCP and the oxygen molecule, the k_p and k_{isc} of TSCP as well as the k_f and k_{ic} of the TSCP-O₂ complex were computed using the MOMAP software. Together with the Jablonski diagram, the results indicated that when the ground state (S_0) of TSCP was excited to the first singlet excited state (S_1), first, the electron arrived at the first triplet state (T_1) via intersystem crossing, and eventually returned to the S_0 state with emission of phosphorescent. However, the ground state of the TSCP-O₂ complex was a spin triplet (T_0). After being excited to the T_1 state, the electron could only undergo internal conversion and returned to the T_0 state without spin flip.

Different from the dynamic collision theory, we proposed a novel quenching mechanism of oxygen sensing based on the photophysical processes discussed above. Three steps are involved in the proposed mechanism. The first step involves the combination of TSCP with oxygen molecules to produce the triplet TSCP-O₂ complex. In the second step, the TSCP-O₂ complex is excited to the triplet excitation state. In the last step the TSCP-O₂ complex in the T_1 state jumped back to the T_0 state through internal conversion. We believe that this new oxygen sensing mechanism would provide excellent theoretical support and guide for designing and developing new, more effective oxygen sensing materials.

Acknowledgements

This work was supported by the National Natural Science Foundation of China, China (Grant Nos. 21677029 and 21606040); the Fundamental Research Funds for the Central Universities, China (DUT18LK26).

References

- J. Lee, D.W.M. Arrigan, D.S. Silvester, Achievement of prolonged oxygen detection in room temperature ionic liquids on mechanically polished platinum screen-printed electrodes, *Anal. Chem.* 88 (2016) 5104–5111.
- K. Presley, J. Hwang, S. Cheong, R. Tilley, J. Collins, M. Viapiano, J. Lannutti, Nanoscale upconversion for oxygen sensing, *Mater. Sci. Eng. C-Mater. Biol. Appl.* 70 (2017) 76–84.
- C. Chu, K. Lin, Y. Tang, A new optical sensor for sensing oxygen based on phase shift detection, *Sens. Actuatur. B-Chem.* 223 (2016) 606–612.
- M. Partridge, S.W. James, R.P. Tatam, Dissolved oxygen sensing using an optical fiber long period grating coated with hemoglobin, *J. Lightwave Technol.* 34 (2016) 4506–4510.
- S.K. Pankaj, C.A. Kelly, C. Bueno-Ferrer, J.P. Kerry, D.B. Papkovsky, P. Bourke, P.J. Cullen, Application of phosphorescent oxygen sensors in in-package dielectric barrier discharge plasma environment, *Innov. Food Sci. Emerg. Technol.* 33 (2016) 234–239.
- L.W. Winkler, Die bestimmung des im wasser gelösten sauerstoffes, *Ber. Dtsch. Chem. Ges.* 21 (1888) 2843.
- L.C. Clark Jr., Monitor and control of blood and tissue oxygen tensions, *Asaio J.* 2 (1956) 41.
- K. Zhang, H. Zhang, W. Li, Y. Tian, S. Li, J. Zhao, Y. Li, PtOEP/PS composite particles based on fluorescent sensor for dissolved oxygen detection, *Mater. Lett.* 172 (2016) 112–115.
- Y. Amao, Probes and polymers for optical sensing of oxygen, *Microchim. Acta* 143 (2003) 1–12.
- X. Yang, Y. Li, A rhenium complex doped in a silica molecular sieve for molecular oxygen sensing: construction and characterization, *Spectrosc. Acta Pt. A-Molec. Biomolec. Spectr.* 153 (2016) 746–753.
- Y. Zhang, J. Zhang, S. Zhang, Luciferin inspired oxygen sensing with alternant change of color and fluorescence, *Dyes Pigment* 138 (2017) 1–6.
- W. Tang, Y. Sun, S. Wang, B. Du, Y. Yin, X. Liu, B. Yang, W. Cao, M. Yu, Pr³⁺-doped (K_{0.5}Na_{0.5})NbO₃ as a high response optical oxygen sensing agent, *J. Mater. Chem. C* 4 (2016) 11508–11513.
- E. Önal, S. Saß, J. Huprin, K. Ertekin, S.Z. Topal, M.U. Kumke, C. Hirel, Lifetime-based oxygen sensing properties of palladium(II) and platinum(II) meso-tetrakis(4-phenylethynyl)phenylporphyrin, *J. Fluoresc.* 27 (2017) 861–868.
- M. Lindgren, B. Minaev, E. Glimsdal, R. Vestberg, R. Westlund, E. Malmström, Electronic states and phosphorescence of dendron functionalized platinum(II) acetylides, *J. Lumines.* 124 (2007) 302–310.
- T. Sung, Y. Lo, Dual sensing of temperature and oxygen using PtTFPP-doped CdSe/SiO₂ core-shell nanoparticles, *Sens. Actuatur. B-Chem.* 173 (2012) 406–413.
- E. Önal, Z. Ay, Z. Yel, K. Ertekin, A.G. Gürek, S.Z. Topal, C. Hirel, Design of oxygen sensing nanomaterial: synthesis, encapsulation of phenylacetylide substituted Pd(II) and Pt(II) meso-tetraphenylporphyrins into poly(1-trimethylsilyl-1-propyne) nanofibers and influence of silver nanoparticles, *RSC Adv.* 6 (2016) 9967–9977.
- C. Liu, X. Song, Z. Wang, J. Qiu, 2-Phenylquinoline-based cyclometalated platinum (II) complexes: synthesis and structure-photoelectric properties relationship in oxygen sensing, *ChemPlusChem* 79 (2014) 1472–1481.
- Y. Xing, C. Liu, X. Song, J. Li, Photostable trifluoromethyl-substituted platinum(II) emitters for continuous monitoring of molecular oxygen, *J. Mater. Chem. C* 3 (2015) 2166–2174.
- C. Liu, X. Song, X. Rao, Y. Xing, Z. Wang, J. Zhao, J. Qiu, Novel triphenylamine-based cyclometalated platinum(II) complexes for efficient luminescent oxygen sensing, *Dyes Pigment* 101 (2014) 85–92.
- A. Mills, A. Graham, C. O'Rourke, A novel, titania sol-gel derived film for luminescence-based oxygen sensing, *Sens. Actuatur. B-Chem.* 190 (2014) 907–912.
- M.J. Frisch, G.W. Trucks, H.B. Schlegel, G.E. Scuseria, M.A. Robb, J.R. Cheeseman, G. Scalmani, V. Barone, B. Mennucci, G.A. Petersson, H. Nakatsuji, M. Caricato, X. Li, H.P. Hratchian, A.F. Izmaylov, J. Bloino, G. Zheng, J.L. Sonnenberg, M. Hada, M. Ehara, K. Toyota, R. Fukuda, J. Hasegawa, M. Ishida, T. Nakajima, Y. Honda, O. Kitao, H. Nakai, T. Vreven, J.A. Montgomery Jr., J.E. Peralta, F. Ogliaro, M.J. Bearpark, J. Heyd, E.N. Brothers, K.N. Kudin, V.N. Staroverov, R. Kobayashi, J. Normand, K. Raghavachari, A.P. Rendell, J.C. Burant, S.S. Iyengar, J. Tomasi, M. Cossi, N. Rega, N.J. Millam, M. Klene, J.E. Knox, J.B. Cross, V. Bakken, C. Adamo, J. Jaramillo, R. Gomperts, R.E. Stratmann, O. Yazyev, A.J. Austin, R. Cammi, C. Pomelli, J.W. Ochterski, R.L. Martin, K. Morokuma, V.G. Zakrzewski, G.A. Voth, P. Salvador, J.J. Dannenberg, S. Dapprich, A.D. Daniels, Ö. Farkas, J.B. Foresman, J.V. Ortiz, J. Cioslowski, D.J. Fox, Gaussian Inc, Wallingford, CT, USA, 2009.
- A. Abkari, I. Chaabane, K. Guidara, DFT (B3LYP/LanL2DZ and B3LYP/6311G + (d, p)) comparative vibrational spectroscopic analysis of organic-inorganic compound bis(4-acetylanilinium) tetrachlorocuprate(II), *Phys. E* 81 (2016) 136–144.
- P.J. Hay, W.R. Wadt, Ab initio effective core potentials for molecular calculations. Potentials for the transition metal atoms Sc to Hg, *J. Chem. Phys.* 82 (1985) 270–283.
- NIST Computational Chemistry Comparison and Benchmark Database, NIST Standard Reference Database Number 101, Release 19, April 2018, Editor: Russell D. Johnson III, <http://cccbdb.nist.gov/>.
- G. Te Velde, F.M. Bickelhaupt, E.J. Baerends, C.F. Guerra, S.J.A. Van Gisbergen, J.G. Snijders, T. Ziegler, Chemistry with ADF, *J. Comput. Chem.* 22 (2001) 931–967.
- C.F. Guerra, J.G. Snijders, G. Te Velde, E.J. Baerends, Towards an order-N DFT method, *Theor. Chem. Acc.* 99 (1998) 391–403.
- Y. Niu, W. Li, Q. Peng, H. Geng, Y. Yi, L. Wang, G. Nan, D. Wang, Z. Shuai, Molecular materials property prediction package (MOMAP) 1.0: a software package for predicting the luminescent properties and mobility of organic functional materials, *Mol. Phys.* 116 (2018) 1078–1090.
- M.J. Paterson, O. Christiansen, F. Jensen, P.R. Ogilby, Overview of theoretical and computational methods applied to the oxygen-organic molecule photosystem, *Photochem. Photobiol.* 82 (2006) 1136–1160.
- P.R. Ogilby, Singlet oxygen: there is indeed something new under the sun, *Chem. Soc. Rev.* 39 (2010) 3181–3209.
- G. Zhao, K. Han, Hydrogen bonding in the electronic excited state, *Accounts Chem. Res.* 45 (2012) 404–413.
- G. Baryshnikov, B. Minaev, H. Ågren, Theory and calculation of the phosphorescence phenomenon, *Chem. Rev.* 117 (2017) 6500–6537.